

Searching for effects beyond SMEFT in flavour physics

Siddhartha Karmakar

Tata Institute of Fundamental Research, Mumbai, India

Based on : arXiv:2305.16007

In collaboration with Susobhan Chattopadhyay and Amol Dighe.

PHOENIX - 2023, IIT Hyderabad

- Motivation
 - Comparison SMEFT, HEFT and LEFT
-
- Preferred regions for semileptonic operators in $b \rightarrow c\tau\bar{\nu}_\tau$ processes.
 - Angular distribution for $\Lambda_b \rightarrow \Lambda_c(\rightarrow \Lambda\pi)\tau\nu_\tau$.
 - Observables that can distinguish effects beyond SMEFT

Standard Model Effective Field Theory (SMEFT) :

$$\mathcal{L}_{\text{SMEFT}} = \mathcal{L}_{\text{SM}} + \frac{1}{\Lambda} C^{(5)} O^{(5)} + \frac{1}{\Lambda^2} \sum_i C_i^{(6)} O_i^{(6)} + \mathcal{O}\left(\frac{1}{\Lambda^3}\right).$$

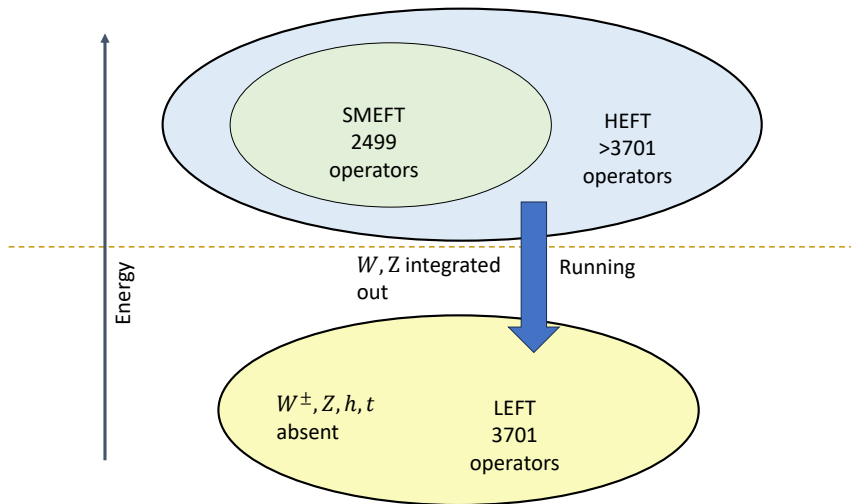
- Includes SM fields only.
- Follows $SU(3)_C \times SU(2)_L \times U(1)_Y$.
- Electroweak (EW) symmetry linearly realized.

Current uncertainties in Higgs coupling measurements allow more generalized EFTs e.g. **Higgs Effective Field Theory (HEFT)**. In HEFT:

- $SU(2)_L \times U(1)_Y$ non-linearly realized.
- Higgs boson is not embedded in a $SU(2)_L$ -doublet: \rightarrow More general coupling of Higgs.
- HEFT \supset SMEFT \supset SM

- In the energy scale much below the EW symmetry breaking, the relevant EFT is **Low Energy Effective Field Theory (LEFT)**
- LEFT can be derived from HEFT by integrating out the heavier particles – W^\pm , Z , Higgs and top quark.

HEFT, SMEFT and LEFT



- Certain EFT operator appears in LEFT but not in SMEFT (at dim-6).
- Example: $\mathcal{O}_V^{LR} \equiv (\bar{\tau}\gamma_\mu P_L \nu_\tau)(\bar{c}\gamma^\mu P_R b)$ which contributes to $R(D^{(*)})$, $R(J/\psi)$, $\Lambda_b \rightarrow \Lambda_c \tau \nu_\tau$ etc.
- Large contribution from $\mathcal{O}_V^{LR} \implies$ non-SMEFT effects.

$$\mathcal{H}_{\text{eff}} = \frac{4G_F V_{cb}}{\sqrt{2}} \left[(1 + g_L)\mathcal{O}_V^{LL} + g_R\mathcal{O}_V^{LR} + g_S\mathcal{O}_S + g_P\mathcal{O}_P + g_T\mathcal{O}_T \right].$$

$$\mathcal{O}_V^{LL} = (\bar{\tau}\gamma_\mu P_L \nu_\tau)(\bar{c}\gamma^\mu P_L b), \quad \mathcal{O}_V^{LR} = (\bar{\tau}\gamma_\mu P_L \nu_\tau)(\bar{c}\gamma^\mu P_R b), \quad (1)$$

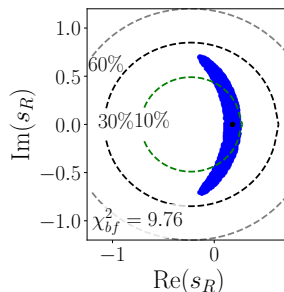
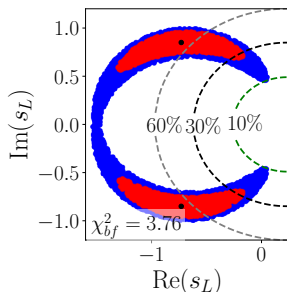
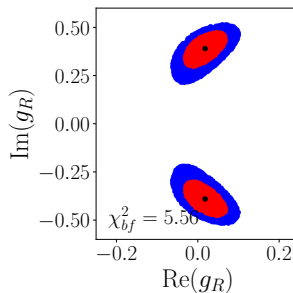
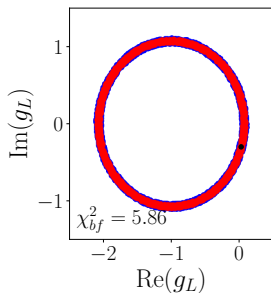
$$\mathcal{O}_S = \frac{1}{2}(\bar{\tau}P_L \nu_\tau)(\bar{c}b), \quad \mathcal{O}_P = \frac{1}{2}(\bar{\tau}P_L \nu_\tau)(\bar{c}\gamma_5 b), \quad (2)$$

$$\mathcal{O}_T = (\bar{\tau}\sigma_{\mu\nu} P_L \nu_\tau)(\bar{c}\sigma^{\mu\nu} b). \quad (3)$$

These operators can contribute to the following observables:

Observables	SM value	Experimental value	Recent updates
R_D	0.298 ± 0.004	0.357 ± 0.029	Belle(2020), LHCb(2023)
R_D^*	0.254 ± 0.005	0.284 ± 0.012	Belle II(2023), LHCb(2023)
$R_{j/\psi}$	0.258 ± 0.004	$0.71 \pm 0.17 \pm 0.18$	LHCb(2018)
$P_\tau^{D^*}$	-0.497 ± 0.013	$-0.38 \pm 0.51 \pm 0.21$	Belle(2017)
$F_L^{D^*}$	0.46 ± 0.04	$0.60 \pm 0.08 \pm 0.035$	Belle(2019)

Scenario	SM	g_L	g_R	s_L	s_R
Best-fit	-	$0.03 - 0.30i$	$0.018 \pm 0.39i$	$-0.73 \pm 0.85i$ <td>$0.18 + 0.00i$</td>	$0.18 + 0.00i$
χ_{bf}^2	22.35	5.86	5.56	3.76	9.76



The branching ratio $\mathcal{B}(B_c \rightarrow \tau \bar{\nu}_\tau)$ puts constraints on the scalar operators.

We consider–

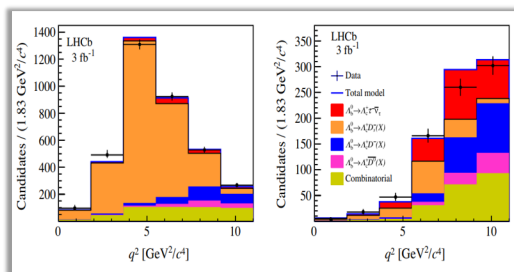
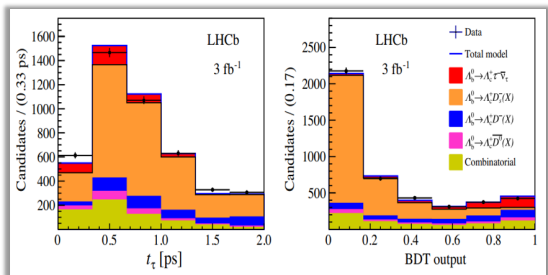
- $\mathcal{B}(B_c \rightarrow \tau \bar{\nu}_\tau) < 30\%$
- $\mathcal{B}(B_c \rightarrow \tau \bar{\nu}_\tau) < 10\%$

Observation of the Decay $\Lambda_b^0 \rightarrow \Lambda_c^+ \tau^- \bar{\nu}_\tau$

 R. Aaij *et al.*^{*}
 (LHCb Collaboration)

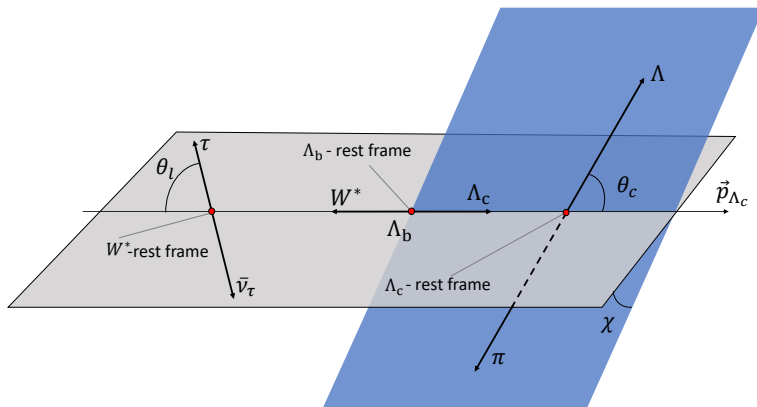
 (Received 11 January 2022; accepted 29 March 2022; published 13 May 2022)

The first observation of the semileptonic b -baryon decay $\Lambda_b^0 \rightarrow \Lambda_c^+ \tau^- \bar{\nu}_\tau$, with a significance of 6.1σ , is reported using a data sample corresponding to 3 fb^{-1} of integrated luminosity, collected by the LHCb experiment at center-of-mass energies of 7 and 8 TeV at the LHC. The τ^- lepton is reconstructed in the hadronic decay to three charged pions. The ratio $\mathcal{K} = \mathcal{B}(\Lambda_b^0 \rightarrow \Lambda_c^+ \tau^- \bar{\nu}_\tau) / \mathcal{B}(\Lambda_b^0 \rightarrow \Lambda_c^+ \pi^- \pi^+ \pi^-)$ is measured to be $2.46 \pm 0.27 \pm 0.40$, where the first uncertainty is statistical and the second systematic. The branching fraction $\mathcal{B}(\Lambda_b^0 \rightarrow \Lambda_c^+ \tau^- \bar{\nu}_\tau) = (1.50 \pm 0.16 \pm 0.25 \pm 0.23)\%$ is obtained, where the third uncertainty is from the external branching fraction of the normalization channel $\Lambda_b^0 \rightarrow \Lambda_c^+ \pi^- \pi^+ \pi^-$. The ratio of semileptonic branching fractions $\mathcal{R}(\Lambda_c^+) \equiv \mathcal{B}(\Lambda_b^0 \rightarrow \Lambda_c^+ \tau^- \bar{\nu}_\tau) / \mathcal{B}(\Lambda_b^0 \rightarrow \Lambda_c^+ \mu^- \bar{\nu}_\mu)$ is derived to be $0.242 \pm 0.026 \pm 0.040 \pm 0.059$, where the external branching fraction uncertainty from the channel $\Lambda_b^0 \rightarrow \Lambda_c^+ \mu^- \bar{\nu}_\mu$ contributes to the last term. This result is in agreement with the standard model prediction.



$\Lambda_b \rightarrow \Lambda_c(\rightarrow \Lambda\pi)\tau\nu_\tau$ angular distribution.

- We consider the process $\Lambda_b \rightarrow \Lambda_c(\rightarrow \Lambda\pi)\tau\nu_\tau$.
- Recently $\Lambda \rightarrow \Lambda_c\tau\nu_\tau$ was observed at LHCb for the first time.
- Angular distribution of the final state particles offer multiple observables to probe the effect of g_R .



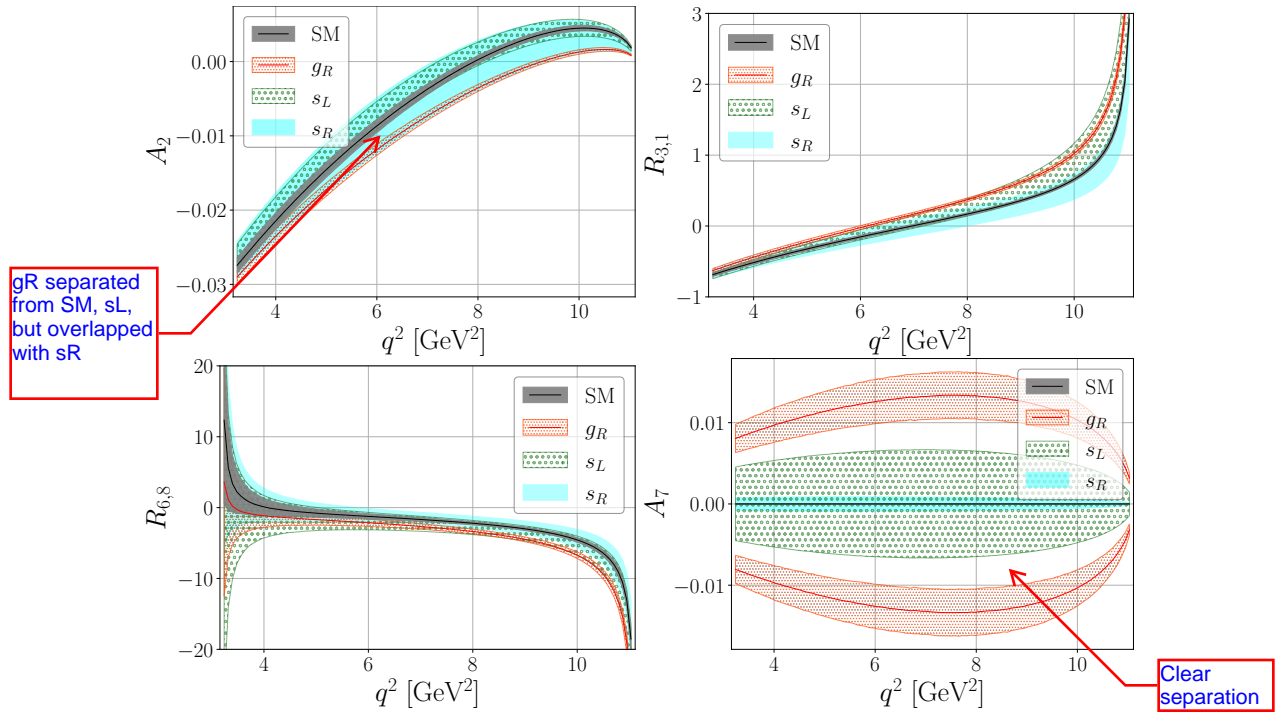
$$\frac{1}{(d\Gamma/dq^2)} \frac{d\Gamma}{dq^2 d\cos\theta_c d\cos\theta_l d\chi}$$

$$= A_0 + A_1 \cos\theta_c + A_2 \cos\theta_l + A_3 \cos\theta_c \cos\theta_l + A_4 \cos^2\theta_l + A_5 \cos\theta_c \cos^2\theta_l$$

$$+ A_6 \sin\theta_c \sin\theta_l \cos\chi + A_7 \sin\theta_c \sin\theta_l \sin\chi + A_8 \sin\theta_c \sin\theta_l \cos\theta_l \cos\chi$$

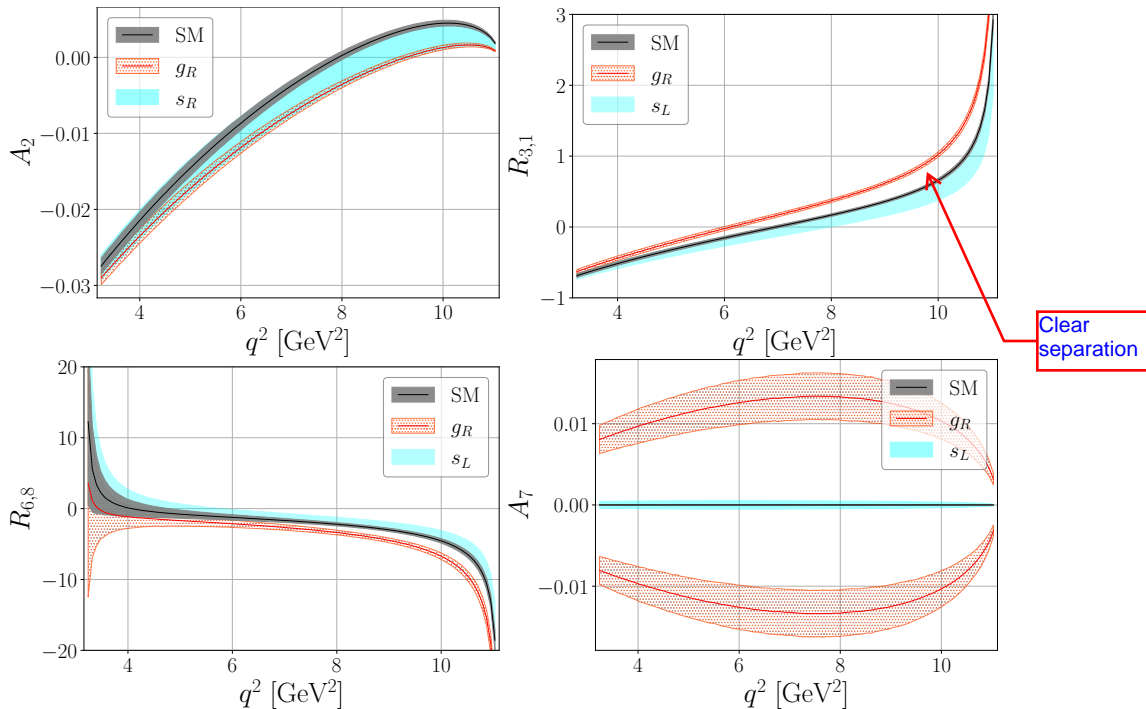
$$+ A_9 \sin\theta_c \sin\theta_l \cos\theta_l \sin\chi .$$

Angular Observables with $\mathcal{B}(B_c \rightarrow \tau \bar{\nu}_\tau) < 30\%$



Angular observables A_2 , $R_{3,1}$, $R_{6,8}$ and A_7 . The values of s_L and s_R are varied within their 2σ allowed ranges, while g_R kept fixed at its best-fit value. For each scenario, 2σ errors from the hadronic form factors and the polarization asymmetry α have been included.

Angular Observables with $\mathcal{B}(B_c \rightarrow \tau \bar{\nu}_\tau) < 10\%$



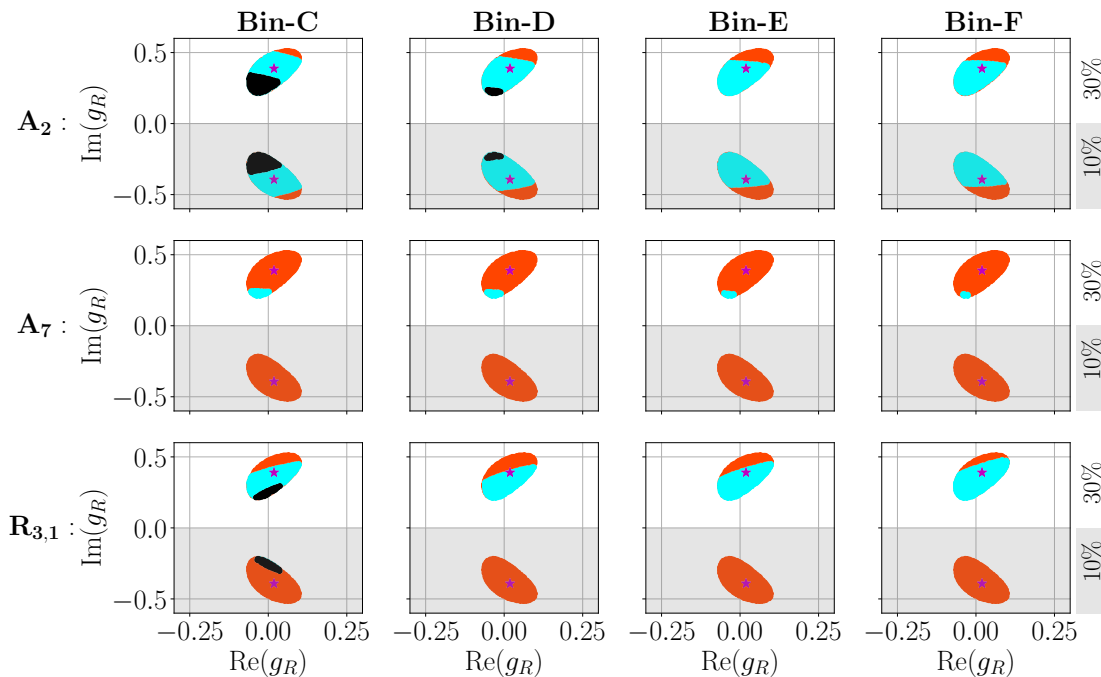
Angular observables A_2 , $R_{3,1}$, $R_{6,8}$ and A_7 . The values of s_L and s_R are varied within their 2σ allowed ranges, while g_R kept fixed at its best-fit value. For each scenario, 2σ errors from the hadronic form factors and the polarization asymmetry α have been included.

Angular Observables

ObservableScenario	$\mathcal{B}(B_c \rightarrow \tau \bar{\nu}_\tau) < 30\%$			$\mathcal{B}(B_c \rightarrow \tau \bar{\nu}_\tau) < 10\%$		
	SM, g_L	s_L	s_R	SM, g_L	s_L	s_R
$d\Gamma/dq^2$	×	×	×	×	✓	×
A_0	×	×	×	×	✓	×
A_1	×	×	×	×	✓	×
A_2	✓	✓ ^(×)	×	✓	✓	×
A_3	✓ ^(×)	×	×	✓ ^(×)	✓	✓ ^(×)
A_4	×	×	×	×	✓	×
A_5	×	×	×	×	✓	×
A_6	×	×	×	×	✓	×
A_7	✓	✓	✓	✓	✓	✓
A_8	×	×	×	×	✓	×
A_3/A_1	✓	×	×	✓	✓	✓
A_3/A_5	✓	✓ ^(×)	×	✓	✓	✓
A_6/A_8	✓	✓ ^(×)	×	✓	✓	✓ ^(×)

The effectiveness of angular observables and their ratios in distinguishing the g_R scenario from the SM and other NP scenarios. Results for $\mathcal{B}(B_c \rightarrow \tau \bar{\nu}_\tau) < 30\%$ and $\mathcal{B}(B_c \rightarrow \tau \bar{\nu}_\tau) < 10\%$ are shown.

Bin-wise possibility of distinguishing g_R contribution



Regions where the g_R scenario can be distinguished from SM, g_L , s_L and s_R (orange), from only SM and g_L (cyan) and from neither (black). Bins C, D, E and F corresponds to q^2 ranges (3.67 – 5.5, 5.50 – 7.33, 7.33 – 9.17, 9.17 – 11.13) GeV².

- Effects beyond SMEFT can be probed indirectly in low energy flavour physics observables.
- We find the effectiveness of different angular observables in $\Lambda_b \rightarrow \Lambda_c(\rightarrow \Lambda\pi)\tau\nu_\tau$ decay which can distinguish non-SMEFT effects from other NP scenarios present within SMEFT.
- It is observed that their effectiveness strongly depends on the constraints on the branching ratio $\mathcal{B}(B_c \rightarrow \tau\bar{\nu}_\tau)$.
- We find that the angular observables A_τ (asymmetry w.r.t the angle between the decay planes) shows the most distinguishable effects coming from non-SMEFT contributions.
- Reduction in the hadronic uncertainties, better constraints on $\mathcal{B}(B_c \rightarrow \tau\bar{\nu}_\tau)$ and precise measurement of Λ_b decay distribution in future will improve the sensitivity of angular observables in understanding the distinct effects of SMEFT vs HEFT and how the $SU(2)_L \times U(1)_Y$ symmetry is realized above EW scale.

- Effects beyond SMEFT can be probed indirectly in low energy flavour physics observables.
- We find the effectiveness of different angular observables in $\Lambda_b \rightarrow \Lambda_c(\rightarrow \Lambda\pi)\tau\nu_\tau$ decay which can distinguish non-SMEFT effects from other NP scenarios present within SMEFT.
- It is observed that their effectiveness strongly depends on the constraints on the branching ratio $\mathcal{B}(B_c \rightarrow \tau\bar{\nu}_\tau)$.
- We find that the angular observables A_τ (asymmetry w.r.t the angle between the decay planes) shows the most distinguishable effects coming from non-SMEFT contributions.
- Reduction in the hadronic uncertainties, better constraints on $\mathcal{B}(B_c \rightarrow \tau\bar{\nu}_\tau)$ and precise measurement of Λ_b decay distribution in future will improve the sensitivity of angular observables in understanding the distinct effects of SMEFT vs HEFT and how the $SU(2)_L \times U(1)_Y$ symmetry is realized above EW scale.

Thank you for your attention!